



Detectors for Imaging and Microanalysis

J Morse, Instrument Support Group, Exp. Div.

School on X-ray Imaging Techniques at the ESRF, Grenoble 5-6 Feb 2007

Overview

- 
- 
1. Some fundamental issues: spatial- and energy- resolution, noise, ...
 2. Detectors in use, properties and limits:
 - i. direct 2D imaging by scintillator-CCD systems
 - ii. (raster imaging) microanalysis with spectrometric semiconductor detectors

Spatially resolving, imaging detectors

‘Spatial Resolution’: some definitions...

For imaging applications, resolution is usually described by the *Modulation Transfer Function* (M), i.e. the system response to a sine-wave spatial-frequency amplitude.

Response of a complex system (e.g. scintillator-lens-sensor) can then be evaluated as simple *product of the individual component MTF's*.

In practice, it is easier to measure **either**

the *Contrast Transfer Function* (C) i.e. the square wave spatial frequency response, related to M by:

$$M(N) = \frac{\pi}{4} \left[C(N) + \frac{C(3N)}{3} - \frac{C(5N)}{5} + \frac{C(7N)}{7} - \dots \right]$$

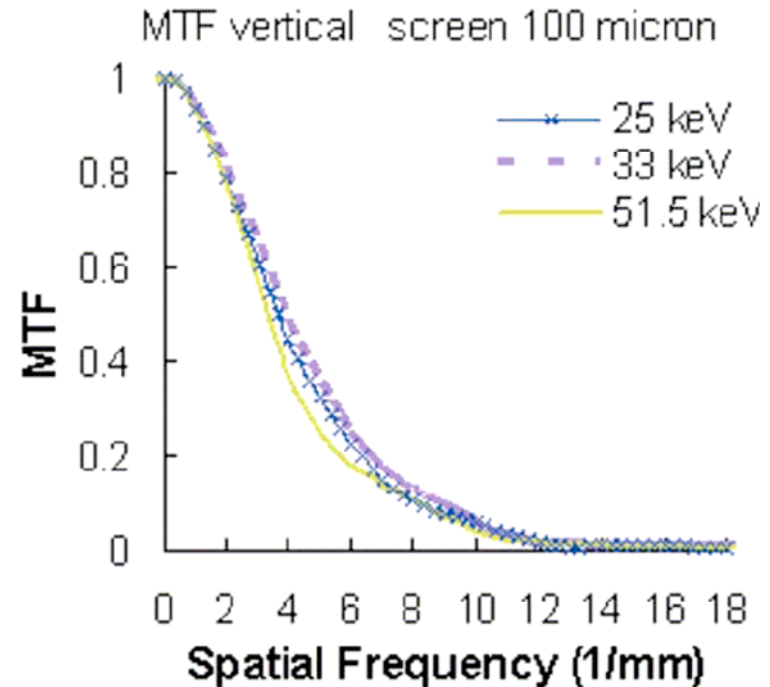
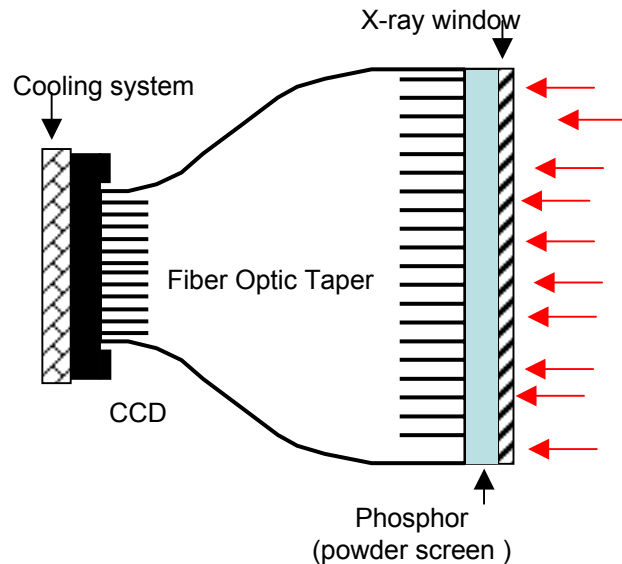
where N is the signal spatial modulation frequency in ‘line pairs’ per unit distance

or

measure the *Line Spread Function* (LSF) i.e. the response of the system to illumination by a narrow slit. The LSF is related to M by the ‘simple’ Fourier transform

$$M(v) = \frac{\left| \sum_{k=-\infty}^{+\infty} \text{LSF}(k \Delta x) e^{-j2\pi vk \Delta x} \right|}{\sum_{k=-\infty}^{+\infty} \text{LSF}(k \Delta x)}$$

Scintillator screen cameras: spatial resolution



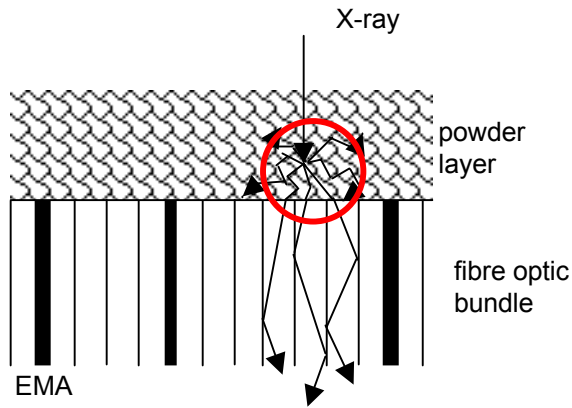
Coan et al., J. Synch Rad, 13 (2006) 260-270

ESRF FReLoN tapered fiber optic camera at ID17: active input surface of 94mm x 94mm, $\text{Gd}_2\text{O}_2\text{S:Tb}$ powder scintillator screen, 3.2:1 demagnification onto $2048^2 \times 14 \mu\text{m}$ pixel CCD effective input pixel size $46 \mu\text{m}$

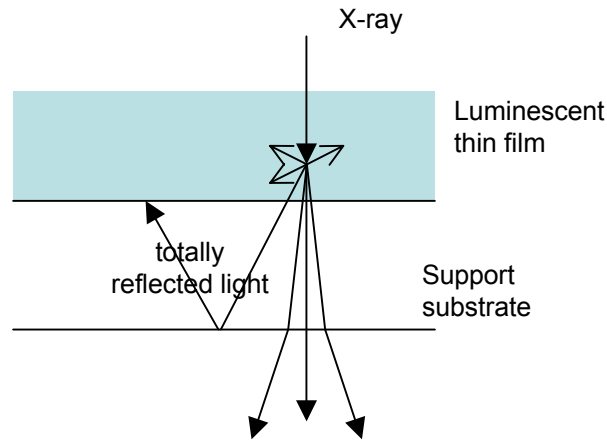
System MTF evaluated from scanning a tungsten blade ('edge spread function' ~ spatial integral of LSF)

Scintillator cameras: screen types

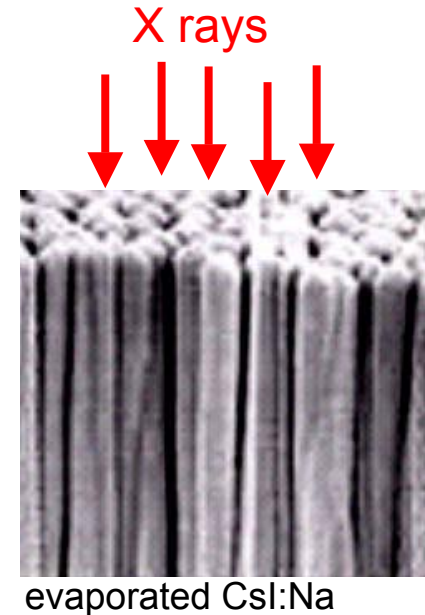
Powder-granular phosphor screen



Crystal screen



'Structured' scintillator

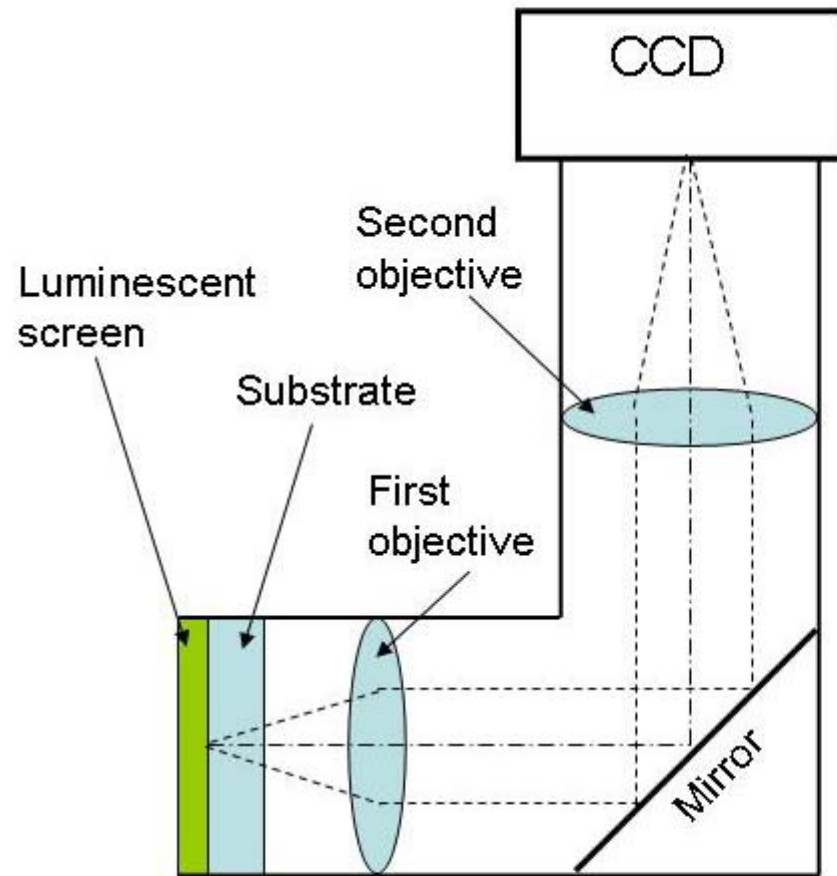


resolution -> few microns fwhm
size -> 50cm

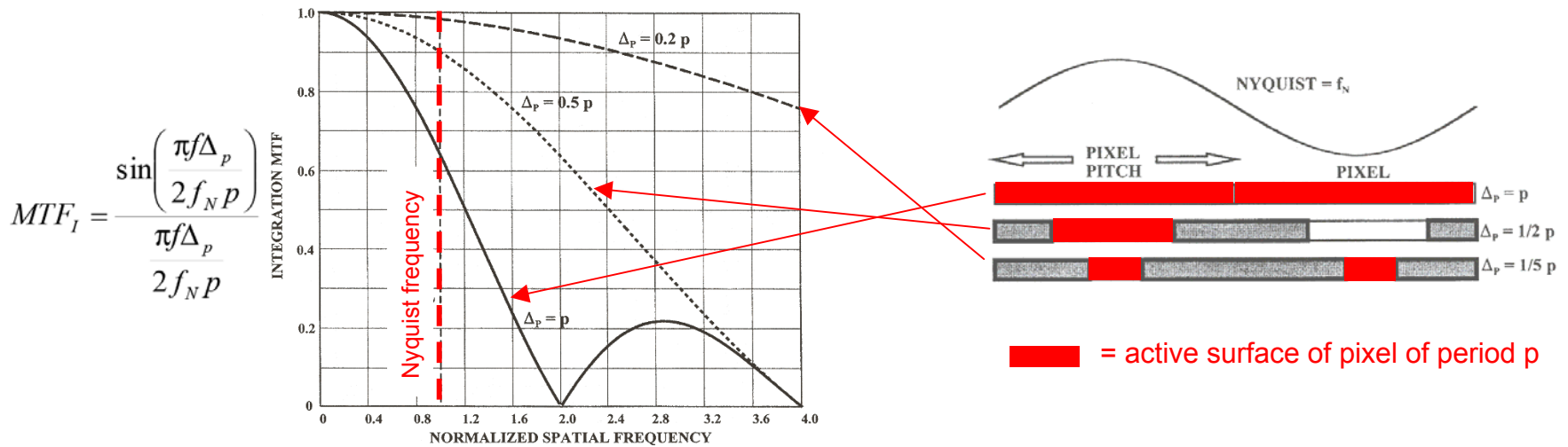
resolution -> $\sim 0.5\mu\text{m}$ fwhm
in 'thin' limit
size $\sim 1\text{cm}$

-spatial artifacts ?
-efficiency ?

Scintillator cameras: crystal screen, high resolution

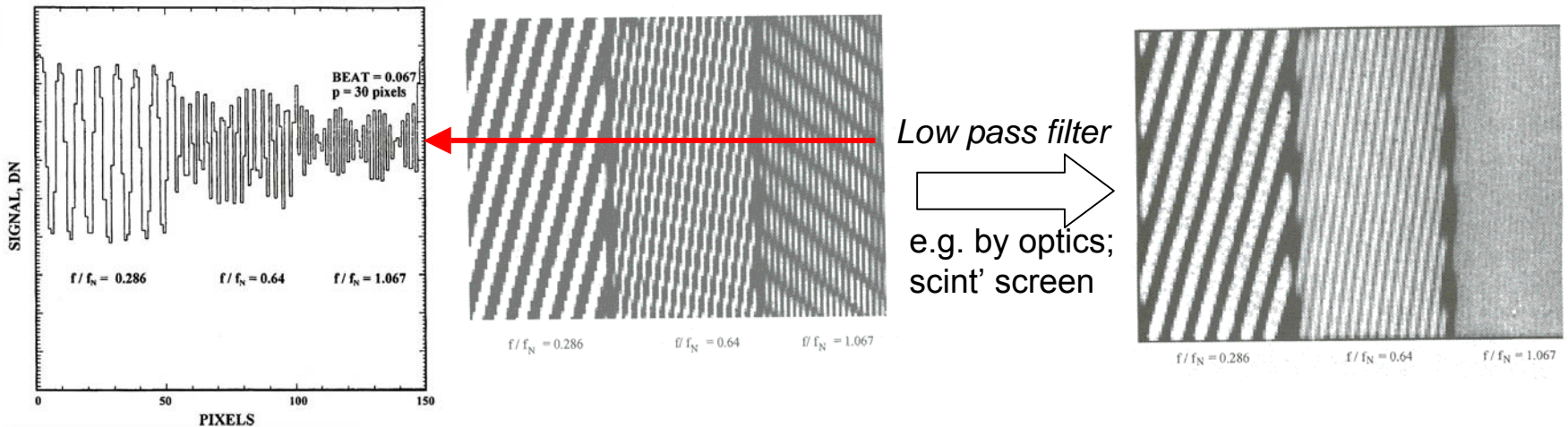


Resolution: imager pixel frequency and fill factor

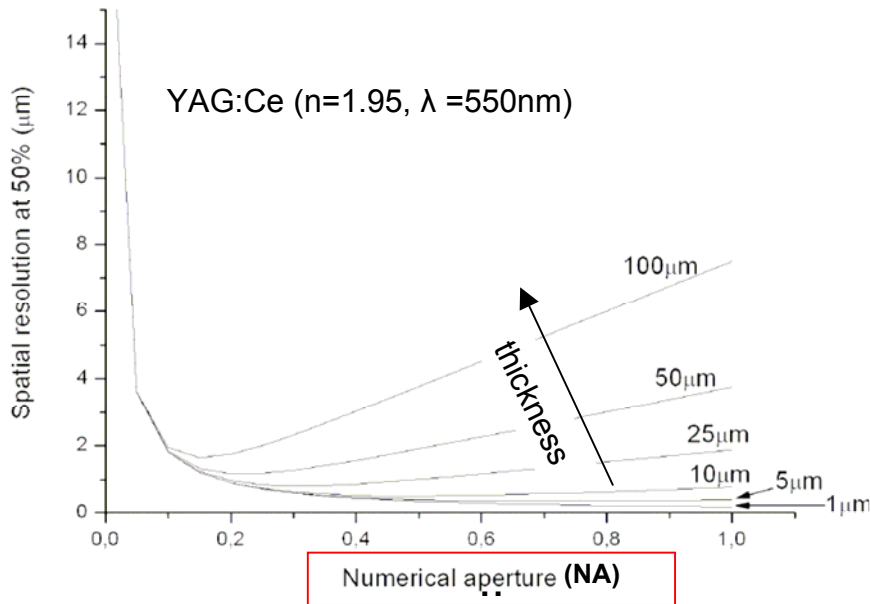


Beating may be observed as *Nyquist sampling limit* is approached.

Nyquist limit: to preserve information, $f_{\text{samp}} (= 1/p)$ must be $>2x$ highest spatial frequencies in image
 Frequencies $> f_N$ are aliased to *false* lower frequencies in the image...



Scintillator cameras: resolution of crystal screen & lens-optic



after Th. Martin/A Koch

from *simple*' optical model, limits to resolution for a crystal screen:

- focus defect $\sim \delta z \cdot \text{NA}$
- Diffraction $\sim \lambda / \text{NA}$
- Spherical aberration $\sim t \cdot \text{NA}^3$

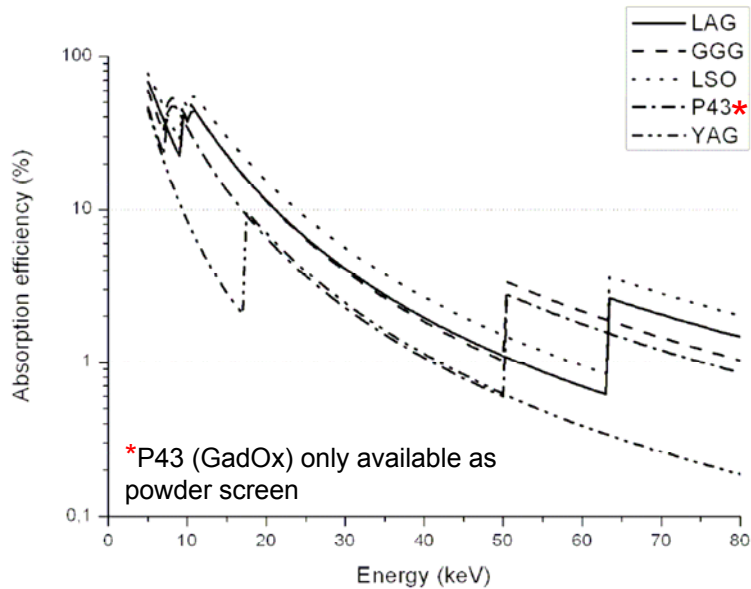
nb. simple analysis ignores:

*photoelectron thermalization range, and **Compton scatter**...*

\Rightarrow *valid only at 'low' X-ray energies*

\Rightarrow *problem of **residual scintillation of substrate** (e.g. YAG:Ce epitaxial film on 'pure' YAG crystal) long range 'tails' to PSF*

Scintillator X-ray Absorption and Light Collection Efficiency, η



Crystal screen + microscope lens:

| Optic | Scintillator | Absorption | DQE | | Spatial resolution (μm) |
|---------------|--------------|------------|--------|-------|--------------------------------------|
| | | | FReLoN | Dalsa | |
| 10x NA=0.3 | YAG:Ce | 0.07 | 0.021 | 0.013 | 2 |
| | LAG:Eu | 0.11 | 0.031 | 0.017 | |
| | GGG:Eu | 0.11 | 0.037 | 0.021 | |
| 20x NA=0.7 | YAG:Ce | 0.07 | 0.049 | 0.038 | 1.04 |
| | LAG:Eu | 0.11 | 0.076 | 0.056 | |
| | GGG:Eu | 0.11 | 0.082 | 0.063 | |

after Th. Martin

calculated for 20keV, and 25 μm thickness scintillator

Scintillator 'quality' factors:

Z, ρ (...refractive index!)

conversion efficiency' (light photons / absorbed X-ray energy)

decay time and *afterglow*

radiation hardness, environmental stability

K edge energy (application dependent)

fabrication feasibility of *thin films* of *optical quality*

Light Collection Efficiency, lens vs. fibre optic bundle

Crystal screen + lens:

$$\eta = \left| \frac{T_L \cdot M^2}{16 \cdot n^2 \cdot f^2 (1+M)^2} \right|$$

Powder screen* + fibre optic:

$$\eta = \left(\frac{1}{m}\right)^2 \cdot \left(\frac{(n_2^2 - n_3^2)^{1/2}}{n_1}\right)^2 \cdot T_F \cdot (1 - L_R) \cdot F_c$$

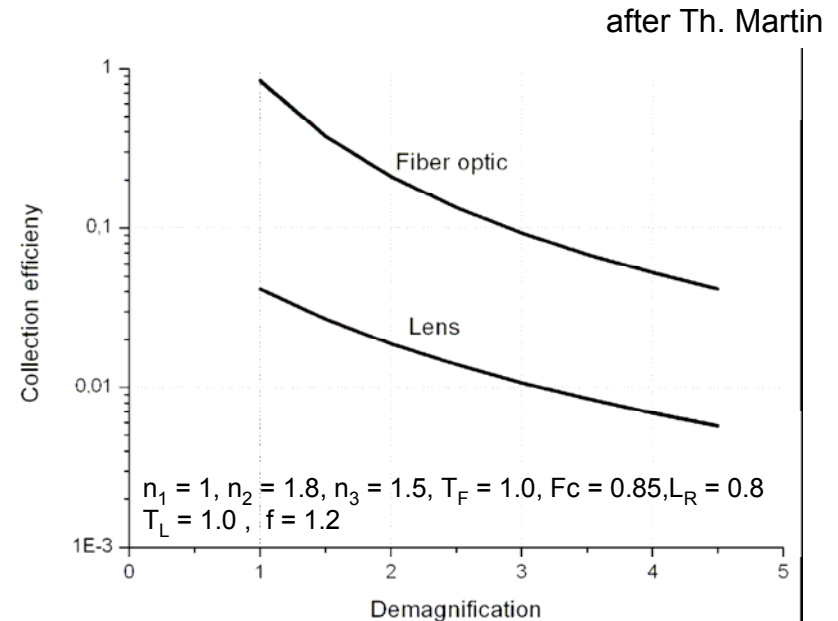
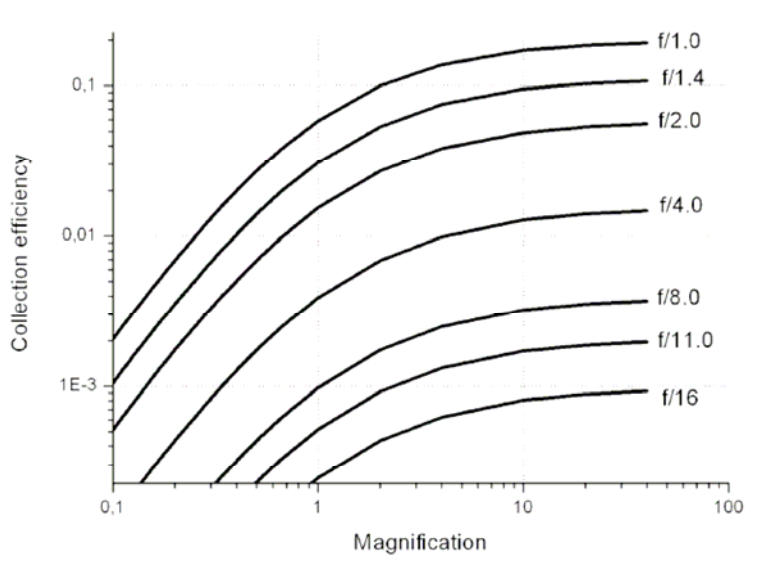
Powder screen* + lens:

$$\eta = \left| \frac{T_L \cdot M^2}{M^2 + 4 \cdot f^2 \cdot (1+M)^2} \right|$$

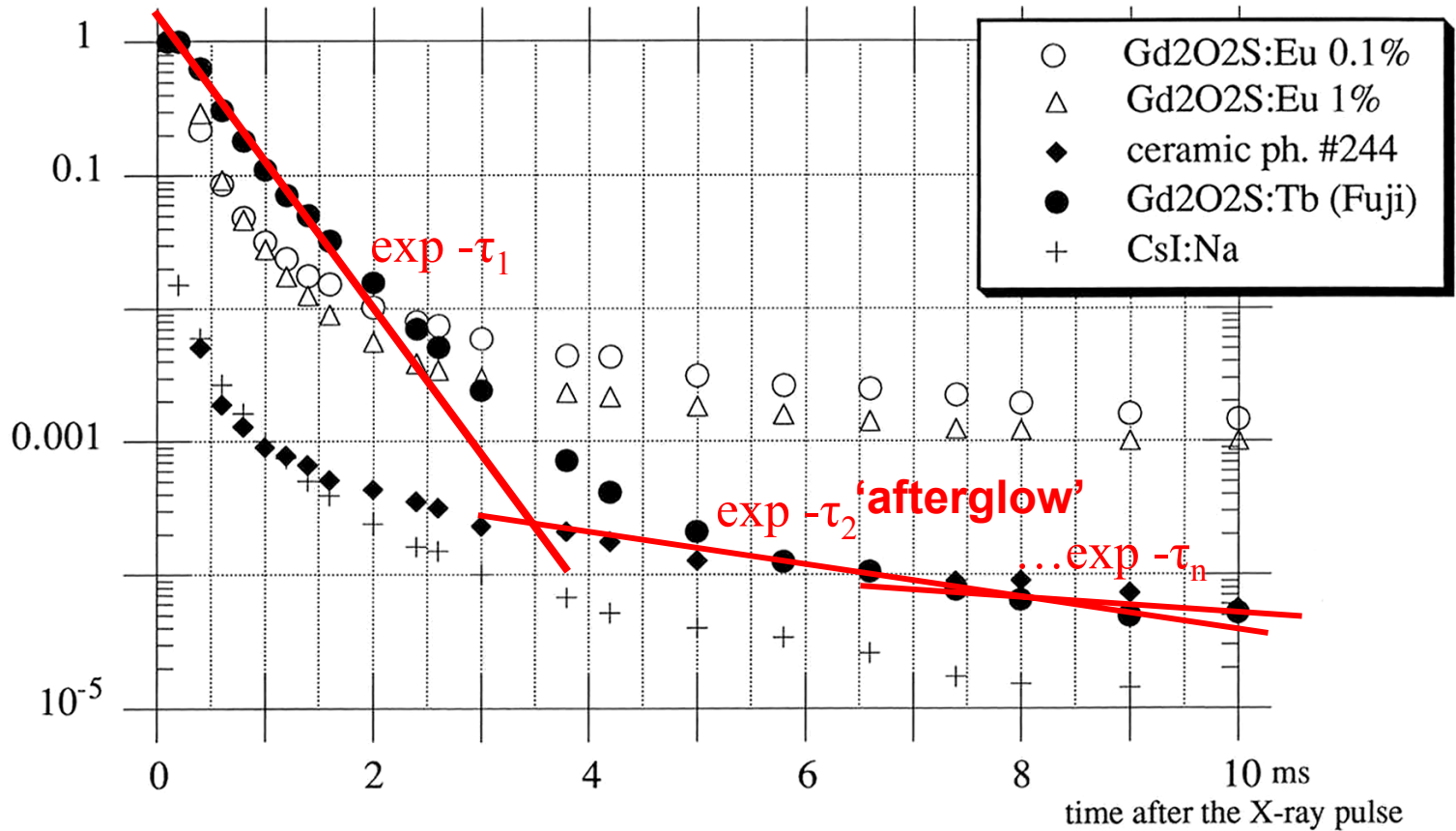
*assumes 'Lambertian' emission, $I(\Theta) \sim I(\cos\Theta)$

M = image/object size; f = Ø lens / focal length

| Magnification | Lens % | Fiber optic % |
|---------------|--------|---------------|
| 20x | 18 | - |
| 10x | 17 | - |
| 4x | 13.7 | - |
| 1x | 4.1 | 84 |
| 0.5 | 1.9 | 21 |
| 0.25 | 0.7 | 6 |

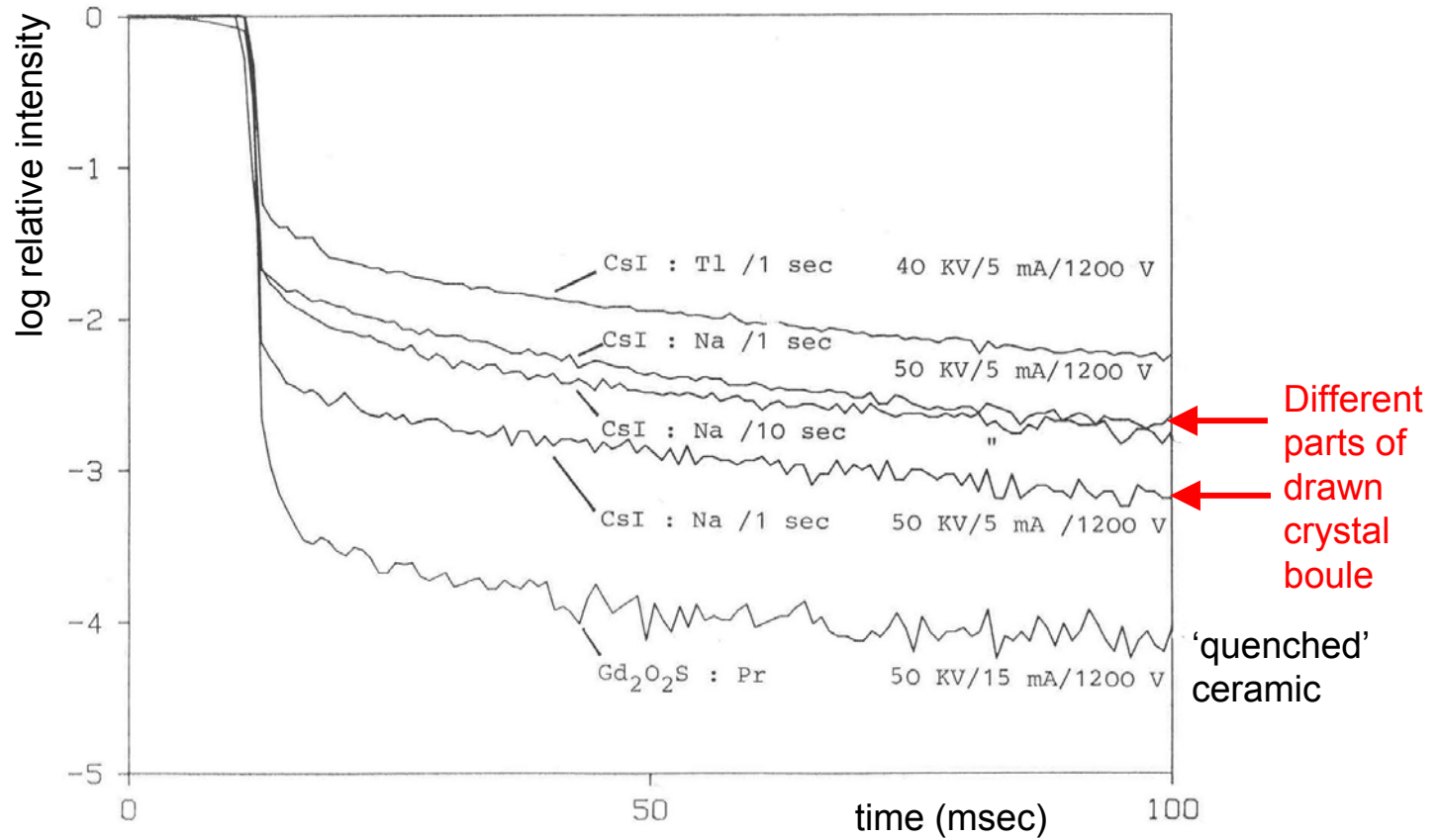


Scintillator time response...



JP Moy et al, NIM A326(1993) 581-586

... the 'afterglow' problem



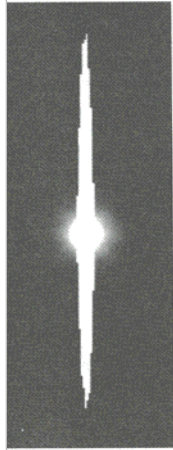
After BC Grabmaier, Siemens 1991

CCD imager basics

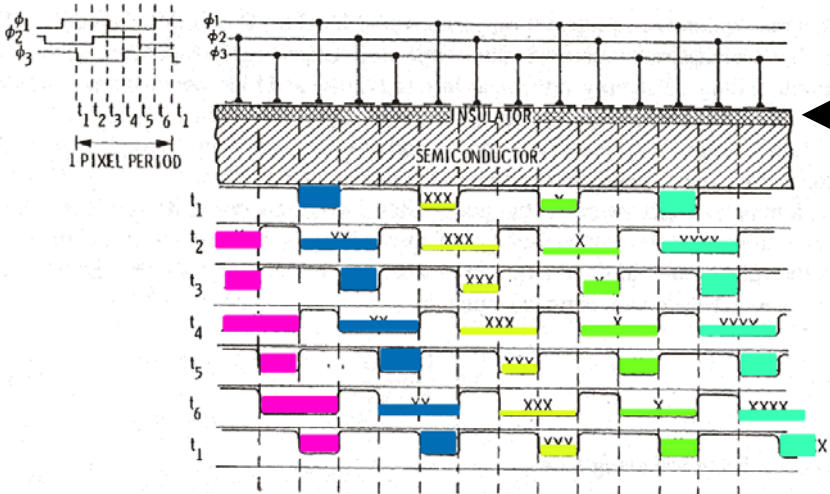
Pixel/buc



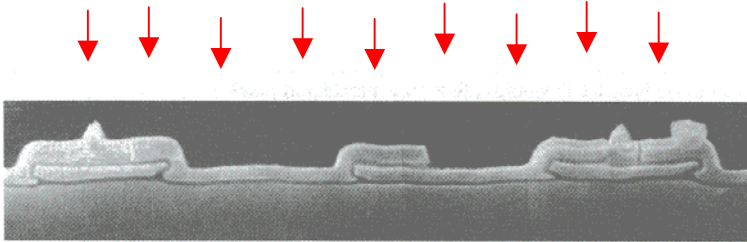
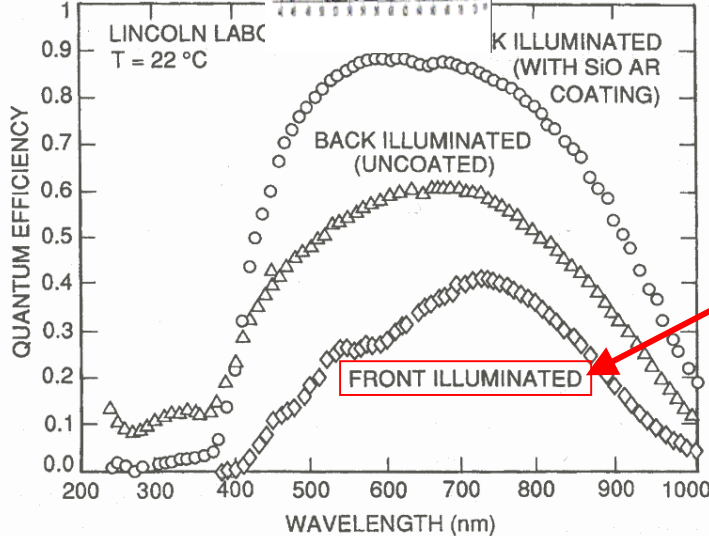
/overflow



GadOx:Tb
CsI:Tl
GadOx:Eu



Charge transfer →

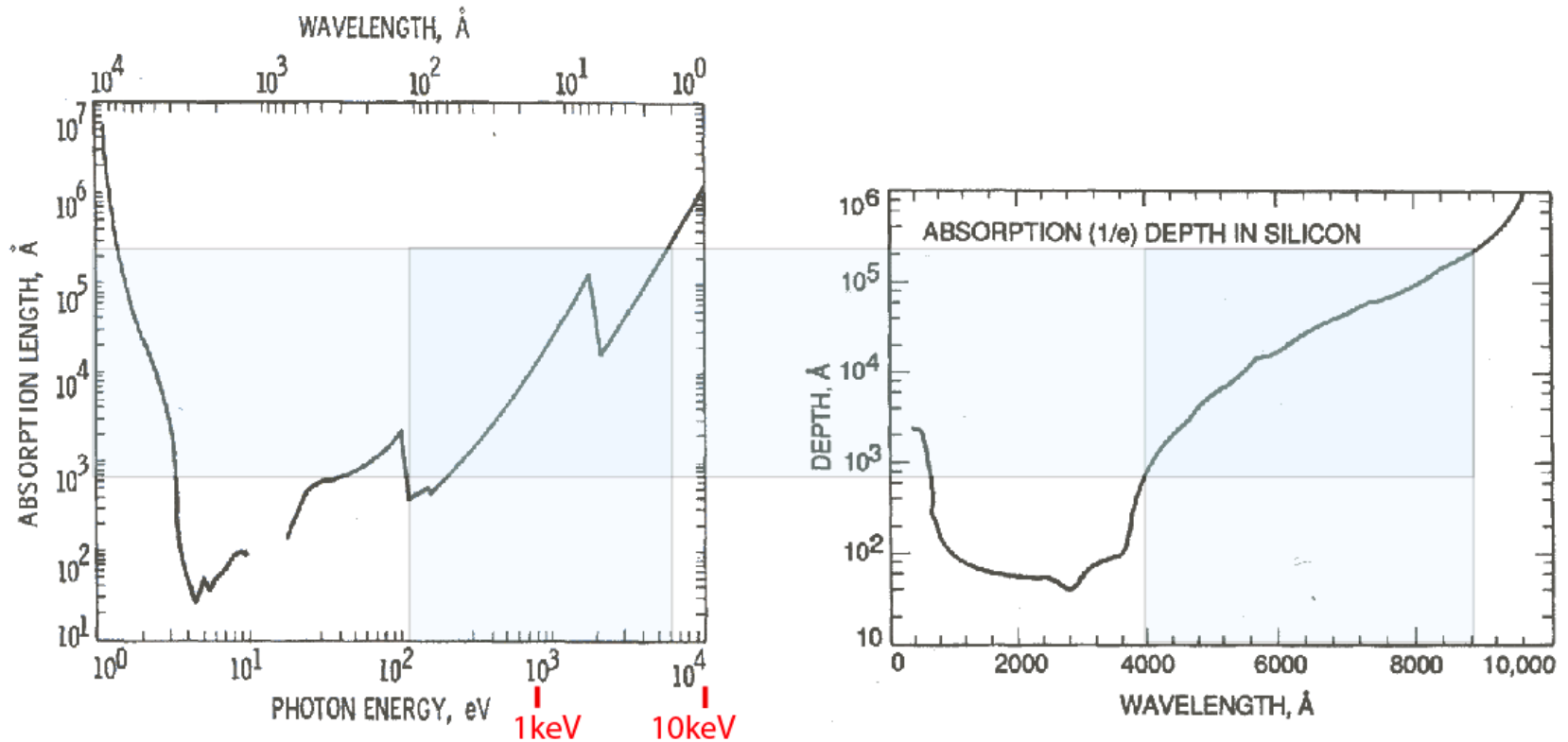


Pixel size ~5...25µm

after J Janesick

CCD: direct X-ray sensitivity

'Fortuitous' overlap of Si absorption length in optical and X-ray bands

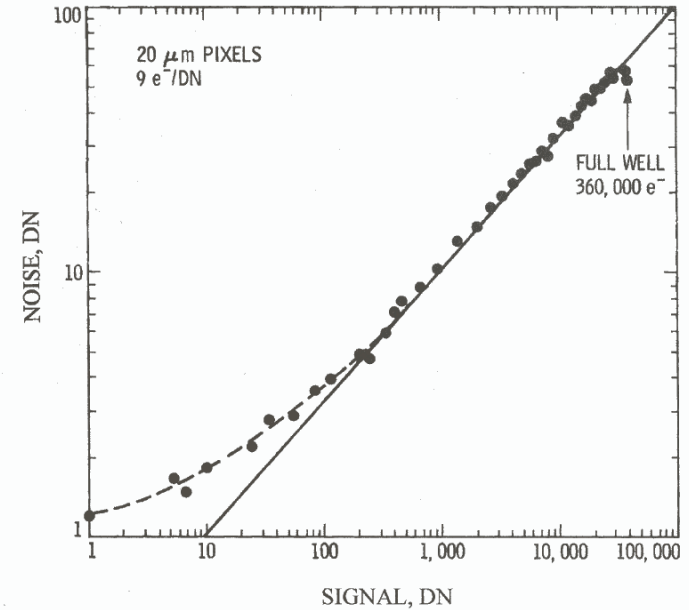
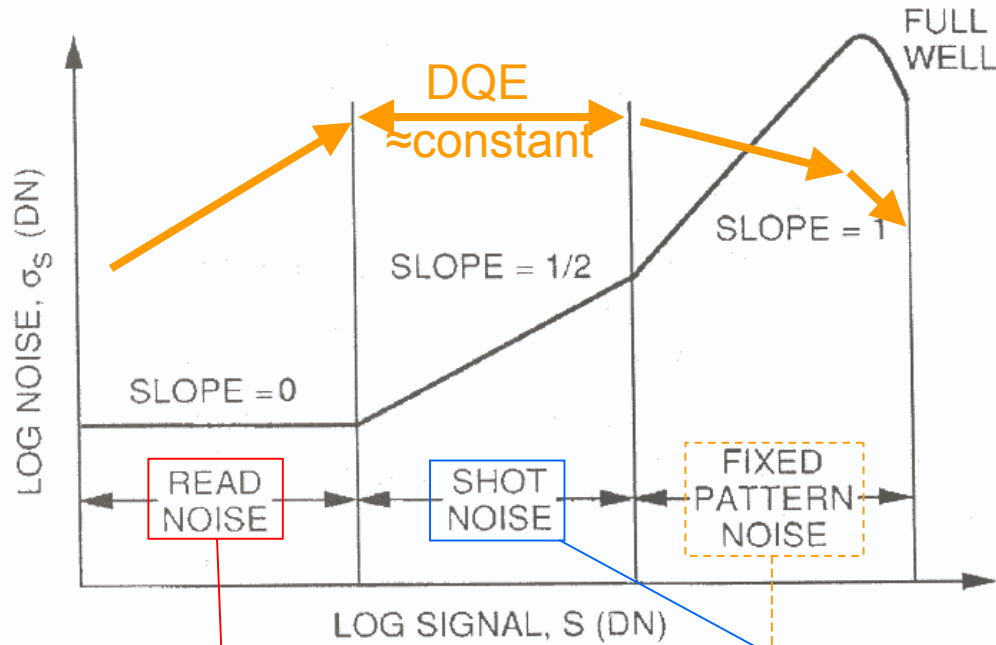


For X-ray sensitive CMOS CCDs, ~100 μm 'active' high resistivity (QE 50% @ 10 keV)
~300 μm for p-n CCD structures

10 keV X-ray generates ~ 2800e⁻ in silicon, ~10% saturation of pixel capacity

⇒ *dynamic range limitation...*

CCD image noise vs. signal



after J Janesick

output MOSFET amplifier white noise and 1/f 'flicker' noise ($f < 1$ MHz)
+ possible 'dark current' offset noise

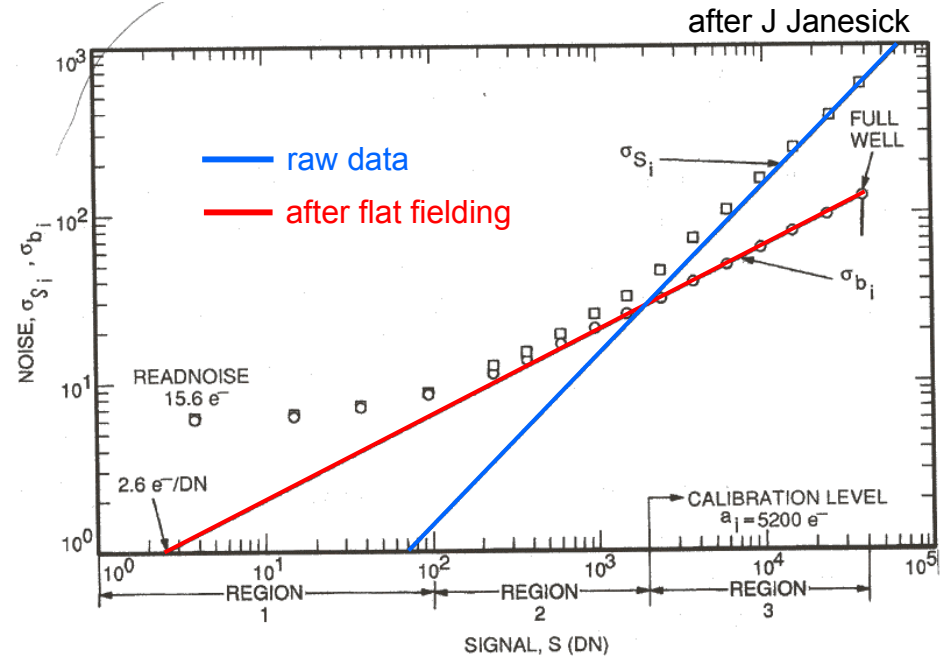
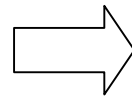
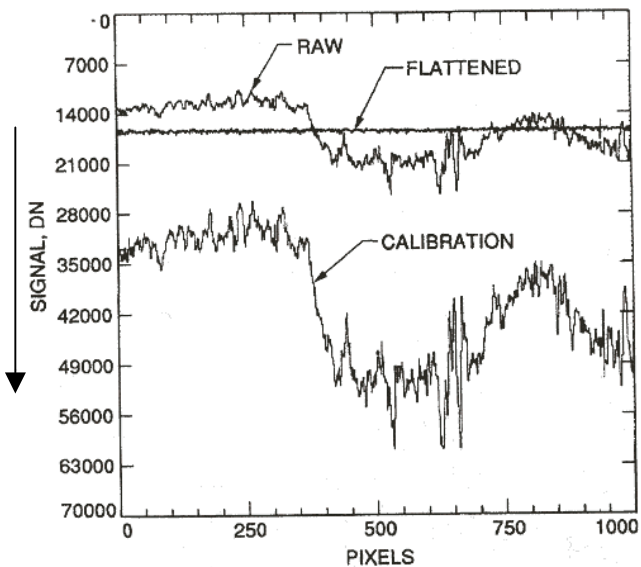
For a 'gain' 8 μ V/e⁻,
noise ~ 10 e⁻ @ 1 MHz = ?? X rays

Reset 'kT/C' noise eliminated
by CDS signal processing

shot noise $\sim \sqrt{N}$ signal electrons
e.g. at 10 000e⁻ (~5% max. CCD signal)
shot noise = 100 (e⁻) = 'signal / noise' ratio

Pixel-pixel efficiency variations
e.g. pixel area variations from CCD
fabrication (mask alignment precision...)

Reduction of CCD (and system) image noise by 'flat field'



multiple (~16) frames acquired and averaged:

- 'dark field' to subtract spatial variations in 'zero' offsets (leakage current offsets)
- 'reference' flat intensity image (ideally, in same exposure conditions as final data image)

Flat fielding errors usually dominant noise for low contrast images

-- difficulty in acquiring accurate reference images:

beam I_0 normalization errors, spatial movements, alignment drifts...

Detective Quantum Efficiency

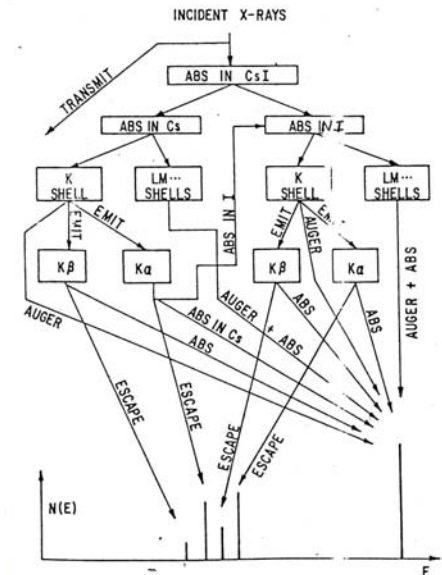
Often quoted 'overall figure of merit' for *any* detector system ('integrating' or photon counting)

$$DQE \equiv \frac{SNR_{out}^2}{SNR_{in}^2}$$

SNR_{in} is the input signal-to-noise ratio (e.g. photon shot noise).

Beware! the effective DQE is a function of many parameters: e.g.

- X-ray energy (phosphor absorption efficiency and *statistics* of cascade processes)
- optical coupling and CCD QE photon-loss statistics
- spatial resolution (MTF) vs. feature integration area
- **signal intensity relative to useful *dynamic range*...**



R Swank, *J. Appl. Phys.* 45 (1974) 4109–203

dynamic range:

For an integrating detector (e.g. CCD), $DR = \frac{\text{signal saturation level}}{(\text{zero signal}) \text{ r.m.s. noise}}$

Do not confuse device dynamic range with obtainable 'signal/noise' :

e.g. for a CCD with pixel saturation level $300ke^-$ and readout noise $10e^-$, $DR = 30\ 000$

but **measuring a $10ke^-$ /pixel signal over a 10 pixel-cluster , CCD signal/noise ≤ 300**

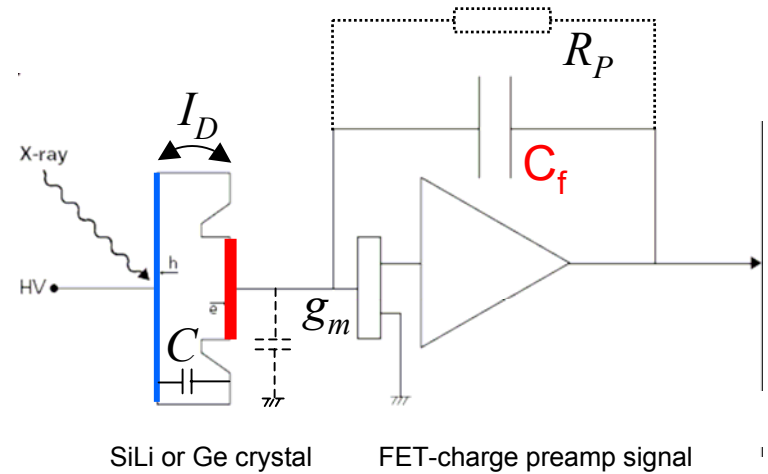
...while for a true 16bit full scale ADC, signal level is coded with a resolution of ~ 1 part in 2000

Spectroscopy: semiconductor detector basics

Cooled crystal of Si or Ge with X-ray transparent rectifying/ohmic contact pair. Strong reverse field completely depletes bulk. Charge q created by X-ray absorption causes step voltage in output of FET charge preamplifier.

$$q = 1.6 \times 10^{-19} E_{\text{xray}}(\text{eV})/3.63 \quad (\text{Si, Coulombs})$$

e.g. for preamp' feedback $C_f=0.1\text{pF}$, a 10keV Xray gives only a 0.5mV signal...



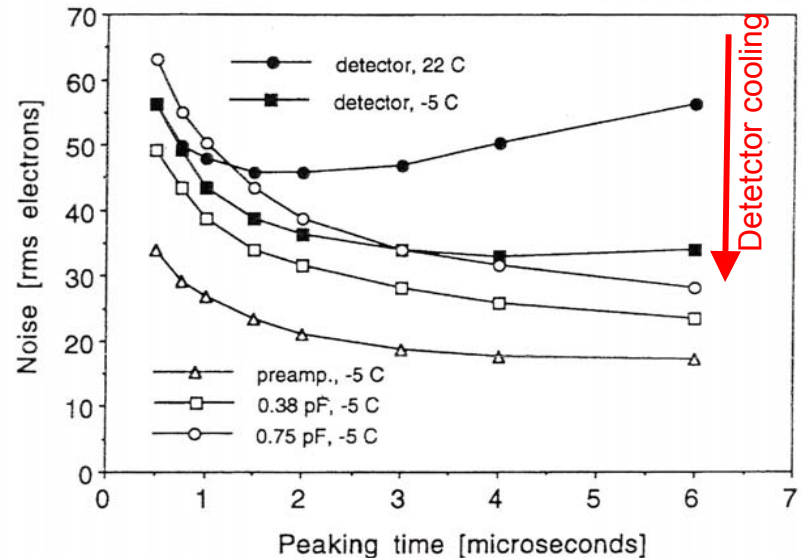
problem is electronic **NOISE**

Equivalent noise charge ENC (e^-) analysis gives

$$ENC \approx \sqrt{\left(\frac{kT}{2R_p} + \frac{eI_D}{4}\right)\tau + \left(\frac{kTC^2}{2g_m}\right)\frac{1}{\tau} + AC^2}$$

Need to:

- maximize R_p ($\rightarrow \infty$ for 'pulse restore' preamp)
- minimize I_D , T (cooling of detector)
- minimize C (crystal geometry, 'drift diode')
- optimize choice of τ** (pulse shaping (peaking) time)



Energy resolution

Generation of electron and hole charges is *statistical process*: energy is shared between lattice excitations (~2/3) and generation of charge carriers (~1/3).

Resultant spread in energy is

$$\text{FWHM} = 2.35 \sqrt{F \epsilon E} \quad \epsilon = 3.63 \text{ eV/e-h for Si}$$

Fano factor $F \approx 0.12$ for Si and Ge (F is *not* a constant)

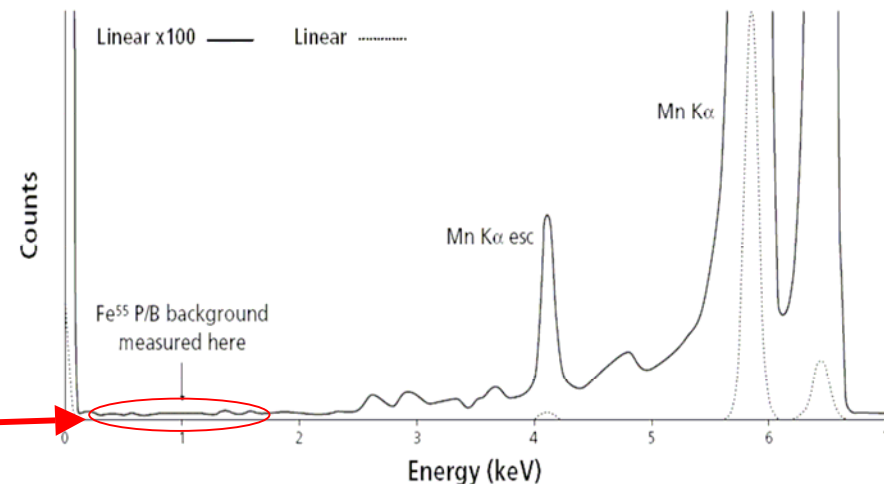
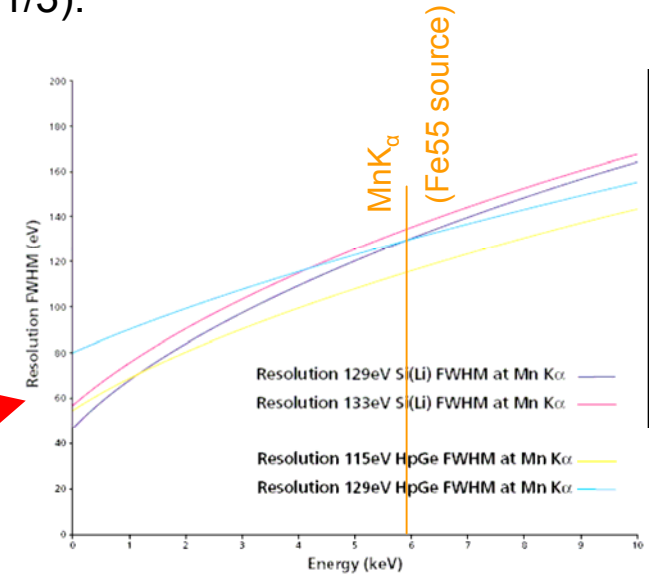
Measured spectral resolution is quadrature-sum of electronic noise and Fano statistics:

$$R = \sqrt{(\text{electronic noise})^2 + (Fano)^2}$$

R should have Gaussian shape, but rarely does at $\leq 1\%$ level... multiple causes:

- near surface X-ray absorptions with incomplete charge collection
- 'ballistic deficit' associated with pulse shaping time
- pulse processor (pile-up and baseline degradation at high count rates)

Peak-valley performance should not be ignored



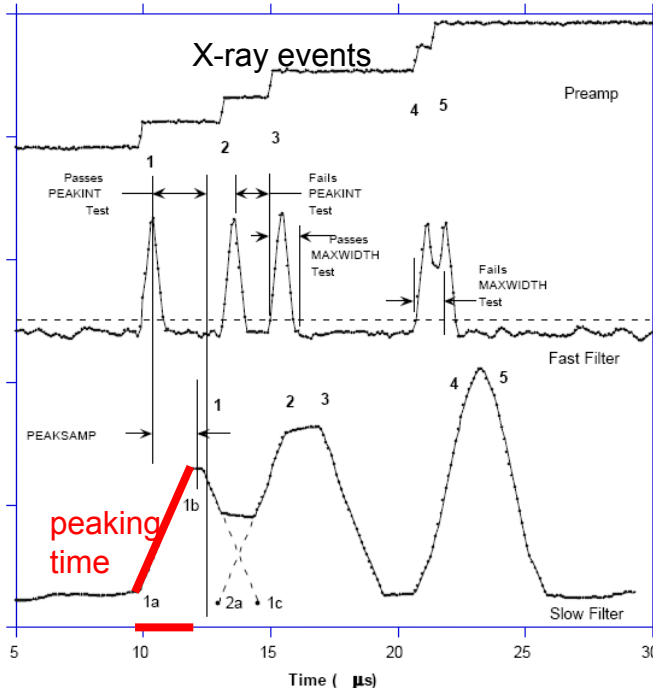
Pulse processing

Spectroscopy pulse processors are 'paralysable': for Poisson time-distributed (?synchrotron?) X-ray events, measured spectrum output count rate can be obtained from

$$\text{ICR} = \text{OCR} \exp(-\text{ICR} \times T_p)$$

T_p is processor 'dead time' associated with processing each event ($\approx 5x$ pulse 'shaping time' or $\approx 2x$ 'peaking time').

Pulse processor optimizes signal/noise with appropriate filter peaking time, detects *pulse pile-up* events and corresponding dead time:



Limits to OCR usually:

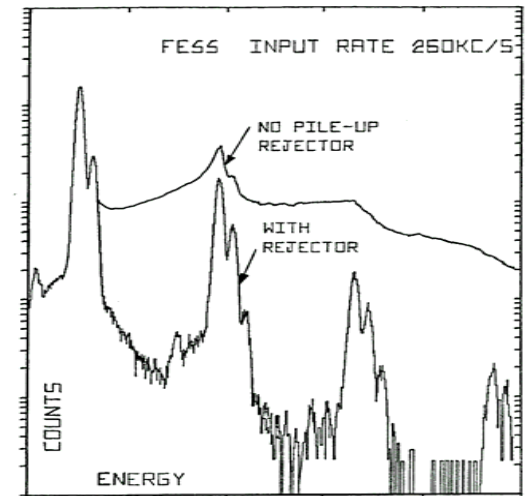
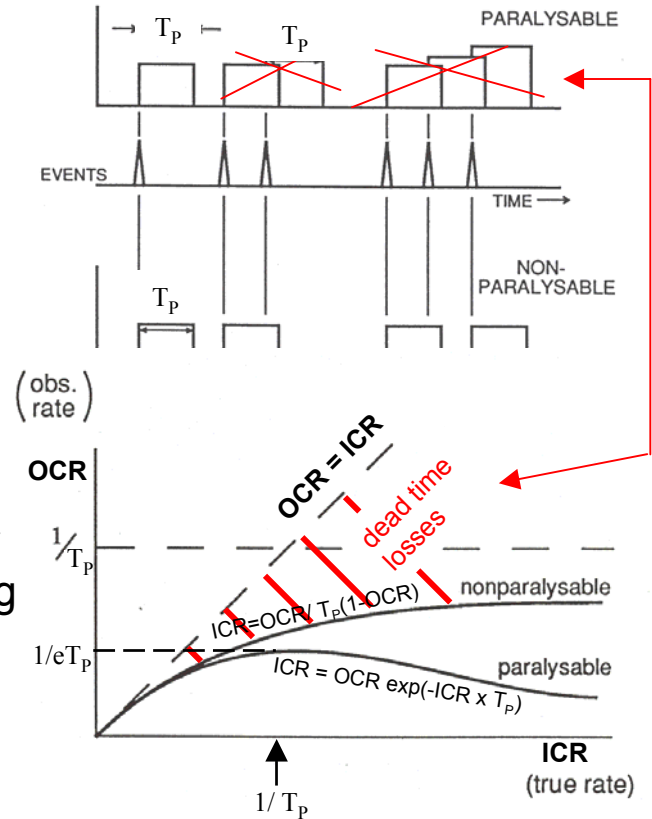
- T_p (energy resolution!)
- detector solid angle

⇒ *multielement systems*

Fast channel
(time info')

slow' channel
(energy)

PUR
→
spectrum



Detector material choice: photopeak efficiency

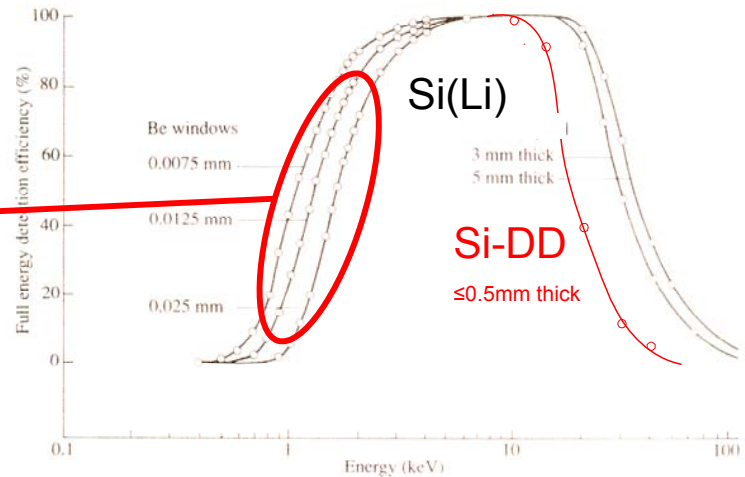
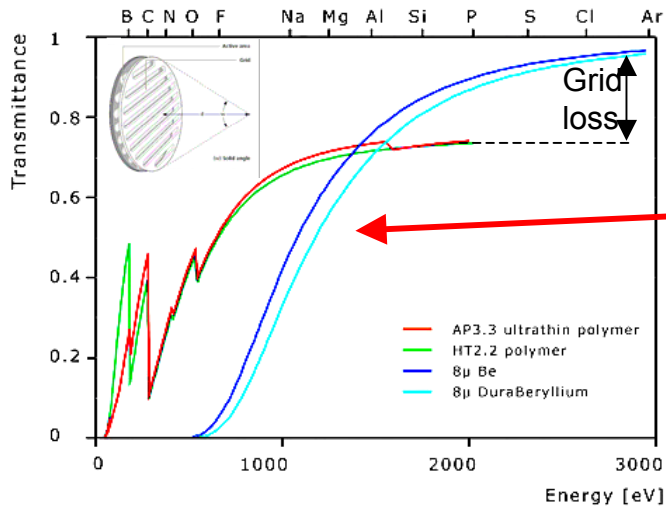
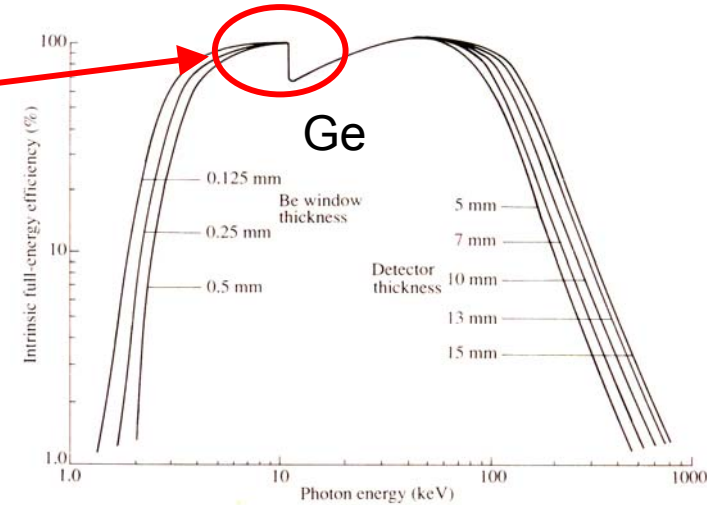
Measured photopeak *intensity* may be reduced due to 'entrance window' (cryostat and detector crystal) absorption losses or fluorescence emission

'Escape' peaks appear at energies ($E_{Xray} - E_{fluor}$)

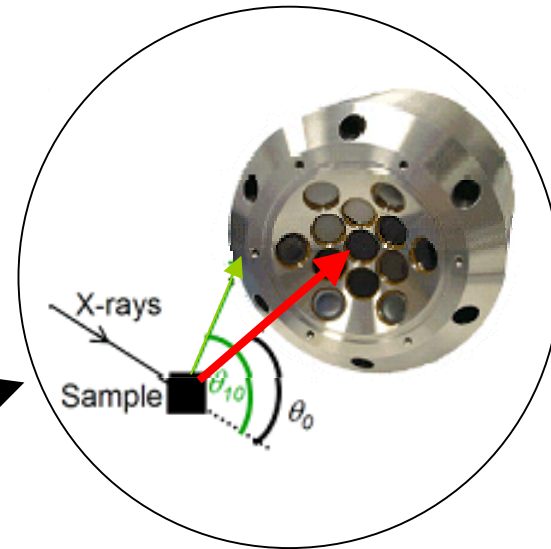
$$\text{where } E_{fluor} \approx 9.9 K_{\alpha}, 1.2 K_{\beta} \text{ Ge} \\ \approx 1.74 K_{\alpha} \text{ Si}$$

Photopeak intensity may be 'smeared' to low energies due to crystal contact/surface loss of electron charge

-> *ultrathin* metal Schottky or epitaxial doped-Si contact technologies

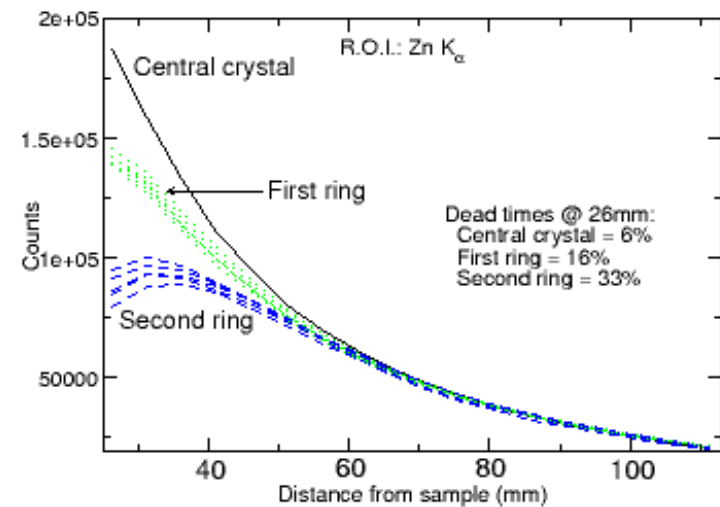
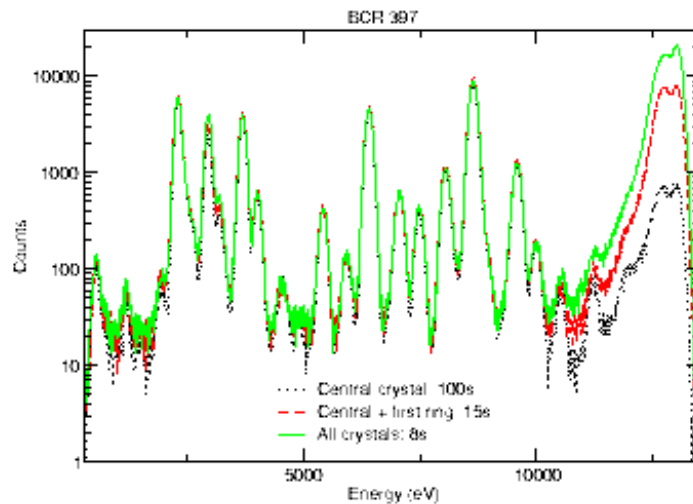


Collection solid angle and beam polarization



higher ratio scatter / fluorescence off-axis...
but overall ~10x counting gain

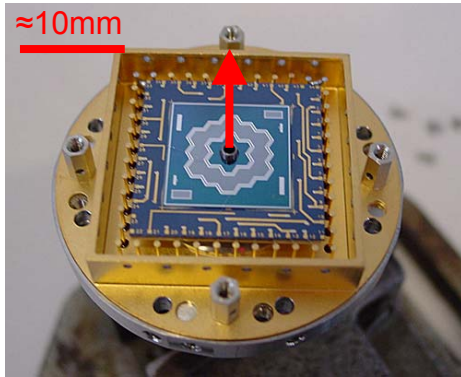
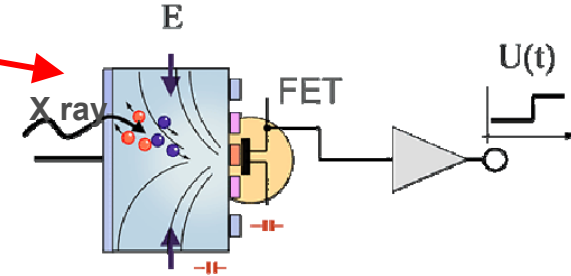
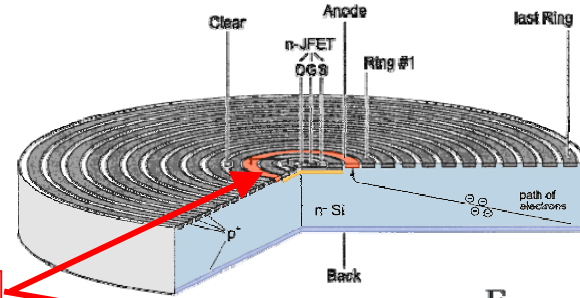
...higher *total* (fluor + scatter count rate) on
off-axis crystals \Rightarrow higher deadtime loss



Silicon Drift Diodes

Planar silicon technology, multielectrodes establish transverse drift field, low capacity charge collecting anode / FET $\sim 100\text{fF}$

Preamp' may be (partly) integrated on detector



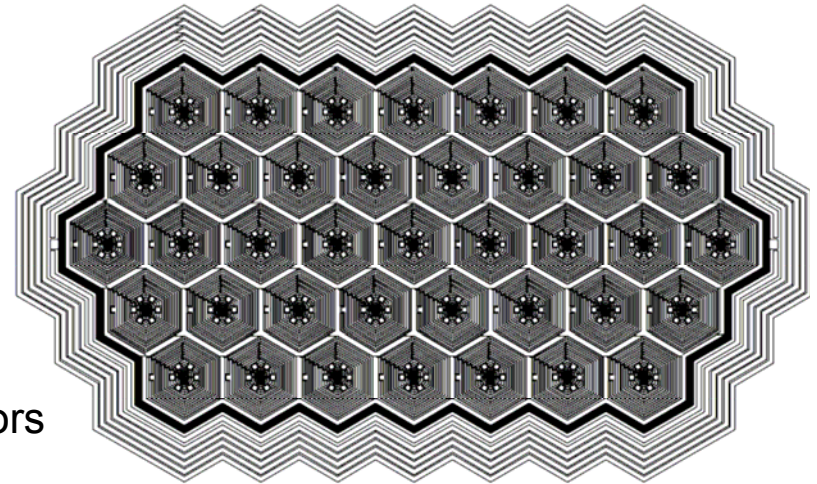
- high resistivity silicon
 - ⇒ low bulk leakage current
 - ⇒ Peltier cooling sufficient $-10^{\circ}\text{C} \dots -50^{\circ}\text{C}$
 - ⇒ *compact, lightweight systems*

Near wafer-scale lithographic processing

large, tightly-packed arrays possible
crosstalk issues

⇒ cell edge effects -> peak/valley limits

- large cell counts
 - ⇒ yield issues
 - ⇒ multi channel pulse processors
 - ⇒ **system cost**



39 cell detector with on-chip FETs, total active area 195mm^2 (after Struder, MPI-Garching)

SII-Vortex Silicon Drift Diode

50mm² area SDD, with discrete JFET

pulse restore operation (~no peak shift with rate)

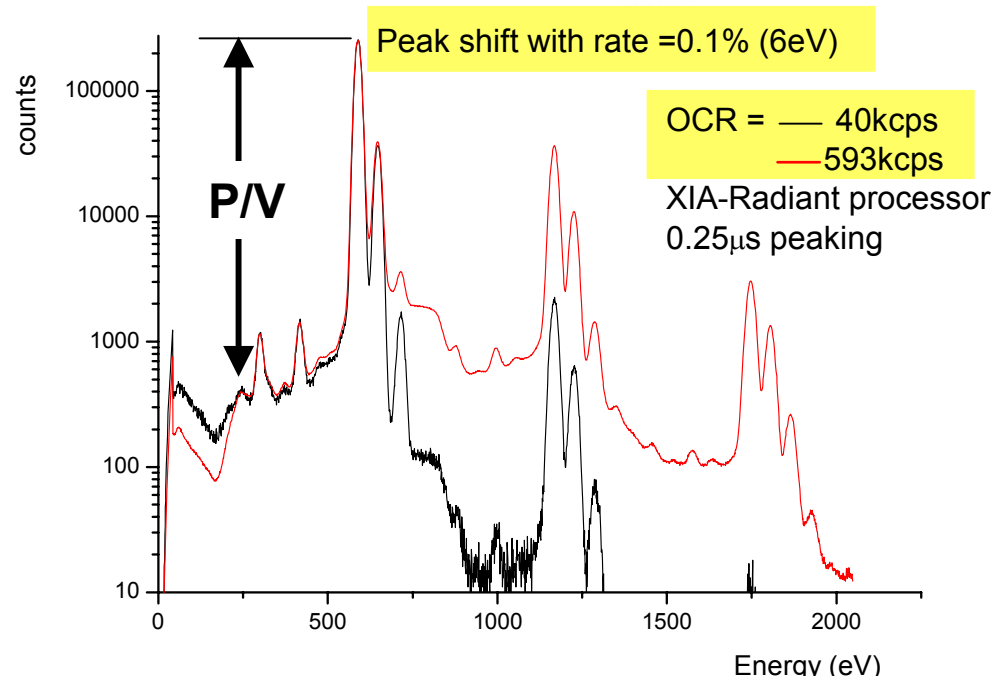
Largest area SDD available for *high rate* applications, now a mature device:

Count rate to ~500kcps possible
(0.25 μ s peaking, 230eV MnK α FWHM)

cf. Si(Li) detector ~25kcps
(5 μ s peaking 160eV MnK α FWHM)

But peak /valley ≤ 700

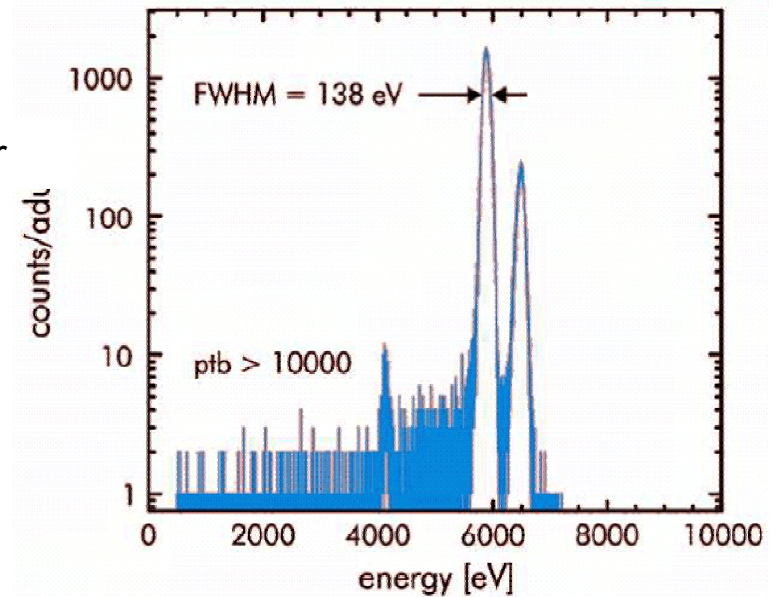
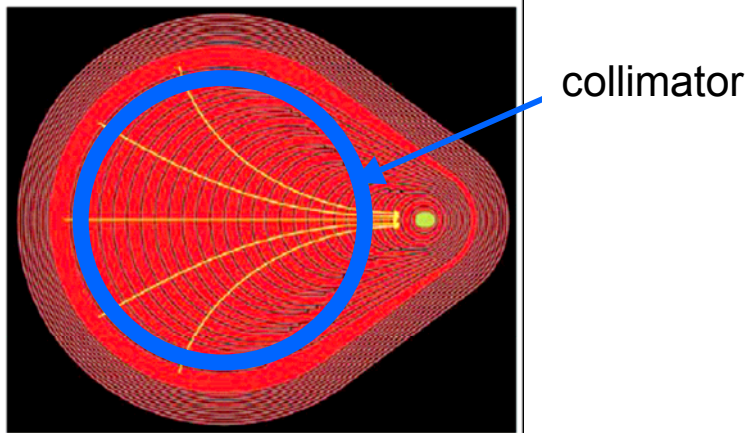
cf. >5000 for Schottky Si(Li) or Schottky Ge



ID21 test data (Mn foil fluo'), ESRF-Diamond

pnSensor 'teardrop' Silicon Drift Diode

Integrated FET structure gives near Fano-limited resolution at low count rates
 but 'continuous' reset mode (now) \Rightarrow noise increase with rate and possible peak shift



Collimator
 protection of FET

\Rightarrow excellent
 peak / valley
 figures

| geometry | active volume | energy resolution FWHM @ 5.9 keV at T = -10 °C | energy resolution FWHM @ 5.9 keV at T = -20 °C | peak/background ratio |
|------------|-----------------------------|--|--|--------------------------|
| symmetric | 5 mm ² x 450 μm | 143 eV - 153 eV | 138 eV - 143 eV | typ. 1.500 |
| symmetric | 10 mm ² x 450 μm | 148 eV - 158 eV | 140 eV - 145 eV | typ. 3.000 |
| symmetric | 20 mm ² x 450 μm | typ. 145 eV | typ. 135 eV | typ. 3.000 - 5.000 |
| symmetric | 30 mm ² x 450 μm | typ. 150 eV | typ. 140 eV | typ. 3.000 - 5.000 |
| asymmetric | 5 mm ² x 450 μm | typ. 145 eV | typ. 133 eV | typ. 7.000 - 10.000 |
| asymmetric | 10 mm ² x 450 μm | typ. 135 eV | typ. 128 eV | typ. 7.000 - 10.000 |

Some bibliography

J Janesick 'Scientific Charge Coupled Devices', SPIE Press, Washington 2001

G Knoll 'Radiation Detection and Measurement', Wiley , 2000

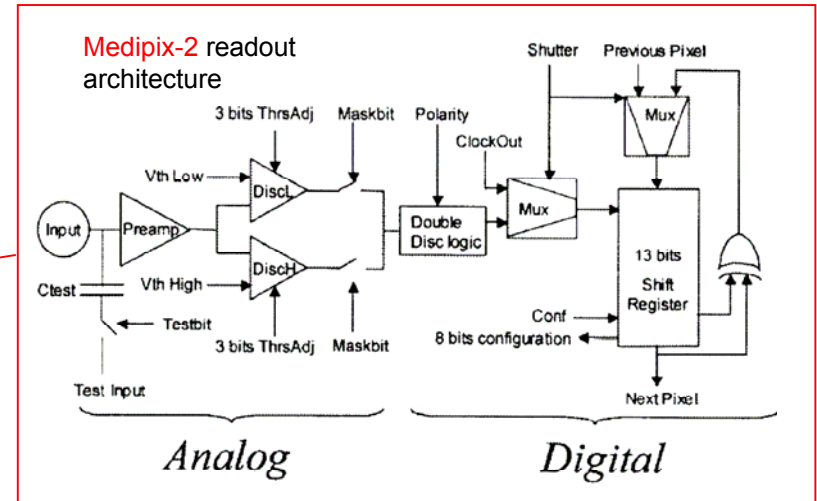
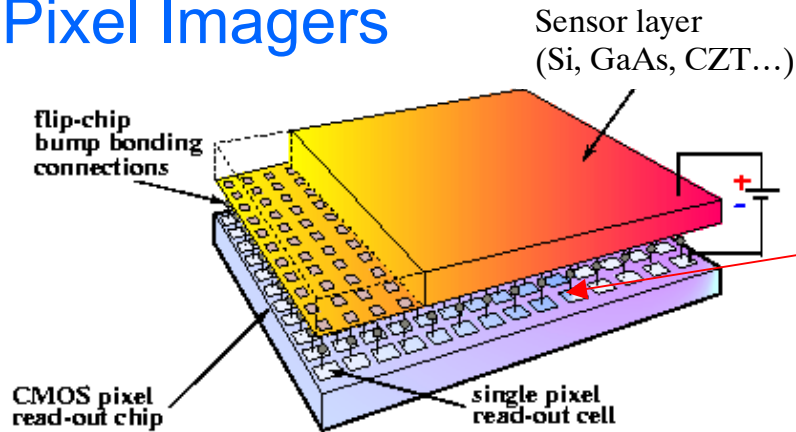
H Spieler, 'Semiconductor Detector Systems', OUP, 2005

C Delaney, E Finch 'Radiation Detectors: Physical Principles and Applications', OUP 1992

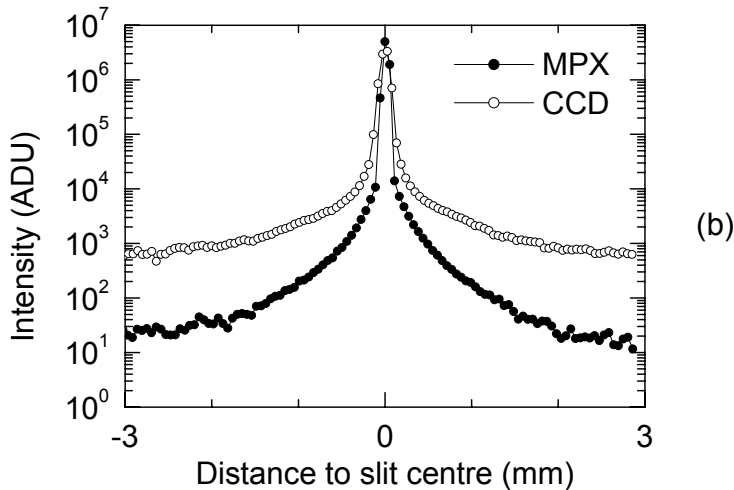
G Lutz, 'Semiconductor Radiation Detectors: Device Physics', Springer Berlin 1999

Postscript-- possible future devices

i. Pixel Imagers



LSF comparison with phosphor-lens coupled CCD(same effective pixel size)



Ponchut et al, IEEE TNS 52 (2005) 1760

55 x 55 μm^2 pixels, 256 x 256 array

300 μm or 700 μm Si sensor layer

13 bits pseudo **counter** at 2MHz,
 \approx 5 keV noise threshold, window discriminator

\approx up to 1000 frames/s with parallel readout

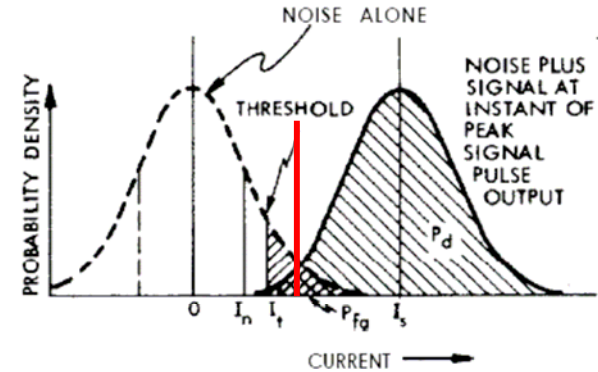
noise free (??)



Photon 'Counting' detectors, noise and background rate

For a 'counting' detector: X-ray event is recognised if above some threshold level set above (electronic) noise floor.

Is it 'noise free' ?

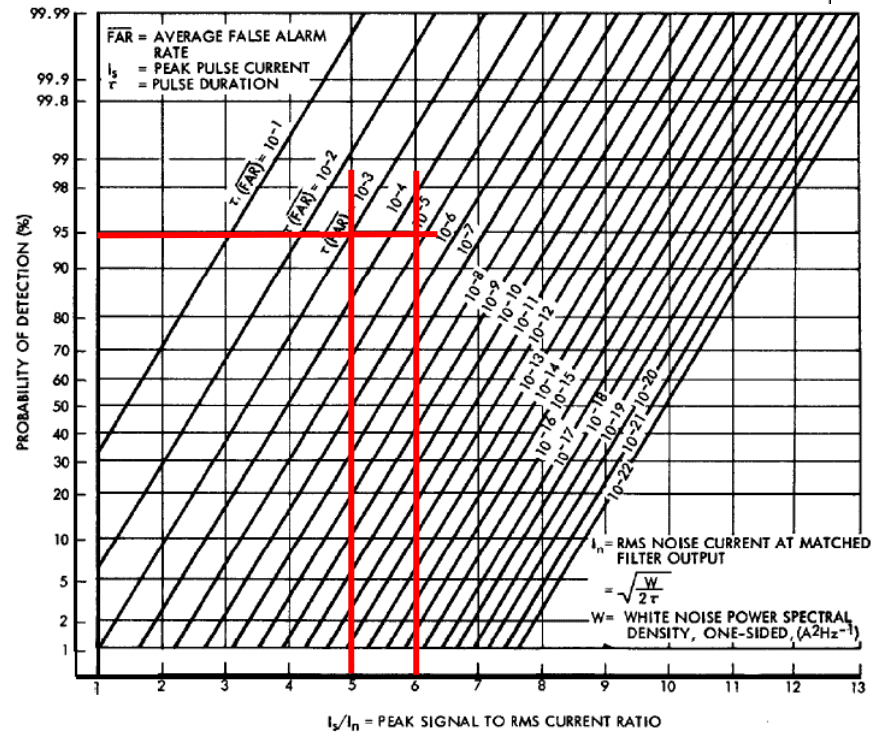


The 'false alarm rate' of noise events is

$$FAR = \frac{1}{2\tau\sqrt{3}} \exp\left(\frac{-I_t^2}{2I_n^2}\right)$$

Consider a 1 sec integration, requiring >95% detection efficiency, for a 1 μsec duration signal pulse in a white noise background

FAR ~500 events/sec for 5σ threshold level
 ~10 events/sec for 6σ



(n.b. this is the 'optimum' case of white noise and matched filter of signal bandwidth = 1/2τ)

ii. DEPFET-macropixel arrays

Matrix arrangement of DEPFET transistor amplifiers at centre of drift diode structure 'macropad' cells .

Various readout possibilities:

direct macropad addressing,

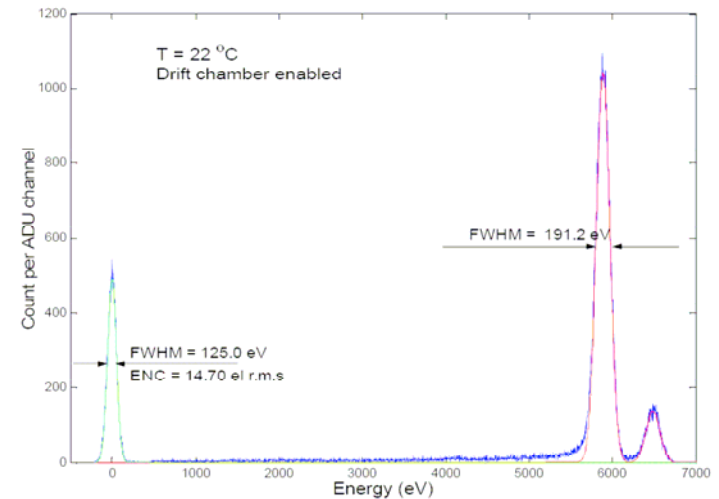
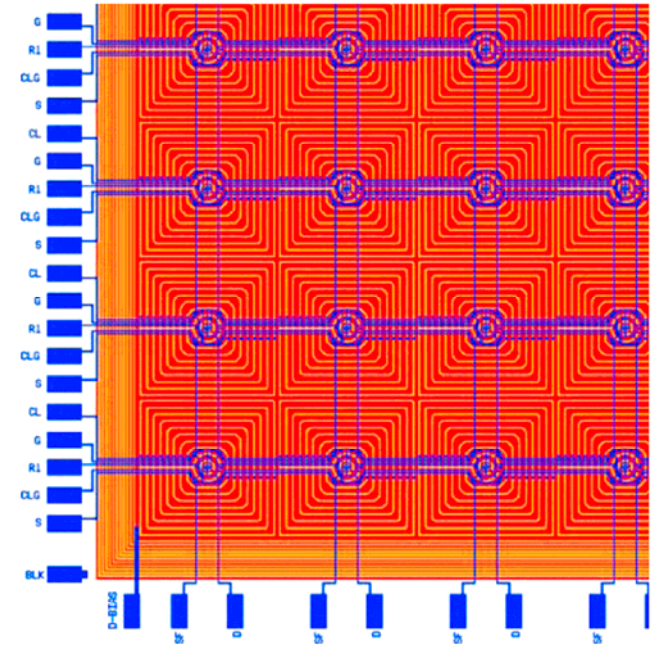
row-by-row readout through single node,

parallel readout of columns (very fast readout)

crosstalk issues?

4 x 4 x 1mm² pixel
prototype

*Room temperature
operation 191 eV !!*



after G Lutz, MPI-Garching & Bonn University